Scientific Research Publishing

Open Journal of Modern Hydrology, 2023, 13, 22-51
https://www.scirp.org/journal/ojmh
ISSN Online: 2163-0496
ISSN Print: 2163-0461

A Framework to Regionalize Flow Information in a Catchment with Limited Hydrological Data

Misigo W. S. Angalika*, Seiji Suzuki, Wataru Tanaka, Huynh V. Vu, Tomoaki Itayama

Department of Advanced Engineering, University, Nagasaki University, Nagasaki City, Japan
Email: *sunfects2010@gmail.com, ssuzuki@nagasaki-u.ac.jp, w.tanaka@nagasaki-u.ac.jp, vuhuynhmt@gmail.com, itayama@nagasaki-u-ac.jp

How to cite this paper: Angalika, M.W.S., Suzuki, S., Tanaka, W., Vu, H.V. and Itayama, T. (2023) A Framework to Regionalize Flow Information in a Catchment with Limited Hydrological Data. *Open Journal of Modern Hydrology*, **13**, 22-51.
https://doi.org/10.4236/ojmh.2023.131002

Received: November 8, 2022
Accepted: January 8, 2023
Published: January 11, 2023

Abstract

This paper describes a framework for mapping flow information from a single gauge to the 9-ungauged river basins with distinct attributes. To establish the basic watershed characteristics at the gauged site, a hydrologic model was calibrated and validated against the historical continuous discharge dataset. The framework was then applied to account for the two watersheds' proportionality in their similarity, such as the influence of land use on transplanting flow signatures to the ungauged site. Three land-use scenarios-discharges at the ungauged and gauged sites formed the basis of an equation mapping the gauged discharge signal to the ungauged site. In comparison with intermittent observed data, the framework prediction attained a precision of $0.85 \geq \text{NSE} \leq 0.95$, $0.80 \geq R^2 \leq 0.94$, $0.56 \geq bR^2 \leq 0.89$. Despite considerable differences in the watershed area, slope, soils, and land cover, the framework satisfactorily depicted the variation in flow pulses at each of the 9 ungauged discharge sites. In the absence of sufficient hydrological information, for example, the presence of a single gauge, the framework provides an alternative method to estimate flow at ungauged sites, reducing uncertainties in the regionalization of model parameters.

Keywords

Prediction, Uncertainty, Regionalization, Mapping, Transplanting Flow Signatures

1. Introduction

The size and structure of watersheds as well as their topographic and geographic structures vary significantly due to geological, morphological, vegetational, soil, and climatic differences [1]. In response to human development, fast climate dynamics, and slow geologic processes, there has been a reciprocal evolution

within catchments resulting in changes in the soils, vegetation, and topography, mediated by material and energy fluxes. This is exhibited in the catchment hydrologic partitioning at the landscape scale and the resulting runoff [2]. Anthropogenic activities by humans often (directly or indirectly) play an important role in altering these landscape characteristics [3] [4]. Quantitative or qualitative flow information is vital for many practical applications. These include water allocation, long-term planning, watershed management operations, flood forecasting, optimization of hydroelectric power production, and hydraulic structure design [5] [6].

Continuous observation of water discharge using the floats or the current meter is impractical, especially on small rivers due to time and resource constraints [7]. Subsequently, the determination of discharge by use of stage height and the stage-discharge rating curve is widely applicable to major rivers that are susceptible to floods or provide vital economic services to the larger ecosystem. In the absence of hydrological data, different approaches have been adopted to try and estimate hydrological aspects of the ungauged watershed using information from the gauged one(s) [8] [9] [10] [11]. One such method is the basic relationship regarding peak discharge at the ungauged site, whereby the gauged data are weighted as a ratio of drainage area with a slope exponent of the curve relating discharge to the watershed area for suitable gauges in the hydrological region [12]. Another technique is the use of a linear correction factor that accounts for the differences in the drainage areas between the gauged and ungauged sites [13]. The flow estimate for the ungauged site is determined by multiplying the correction factor for the ungauged site by the regional regression estimate for the gauged site. These could be applied to the drainage area of the ungauged site that has similar watershed characteristics and area ratios of 0.5 to 1.5. The use of the regional flow duration curve (FDC) has also been employed in the calibration of the ungauged sites [14]. However, the limitation of this method is that the absence of intangible flow timing information affects predictability in ungauged catchments [15].

Since the watershed differs appreciably in weather conditions, topography, vegetative cover, and geology, other researchers have utilized the spatial proximity and regression-based approaches to predict the flow characteristics of a river basin [8] [16] [17] [18]. The accuracy and validity of such flow estimates are directly hinged on the similarity of watershed characteristics (precipitation, drainage area and shape, orographic expression, aspect, vegetation, and lithology/geology) [19] [20]. The estimates at the ungauged sites can be traced back to the origin of the design flow at the ungauged site. Some researchers have determined discharge at the ungauged site by weighting the gauged data by the ratio of the drainage areas and multiplying by an exponent [19]. The exponent was the power function relating discharge to the watershed area (determined by regional regression of the flood region). Other researchers, [14] [21] recommended a different method using a linear correction factor for the difference in the

drainage areas between the gauged and ungauged sites. In hydrologic regions [14] numerous gauges, regression equations have been developed and applied to extrapolate hydrologic information to the ungauged sites within such watersheds [22] [23].

The rainfall-runoff process is a complex, dynamic, and nonlinear process that is governed by multiple, often interrelated physicochemical factors [24]. The hydrologic model approach is widely used to quantify and qualify continuous flow of the rivers in response to human activities in the watershed [6] [25] [26]. Hydrologic models can provide information about rainfall-runoff processes in watersheds, although they remain abstractions of a real system. Any of these models cannot be assumed to exclusively provide accurate information about specific river basins and hydrologic conditions [27]. There are uncertainties in the direct implementation of hydrologic models at the ungauged catchments. One of the challenges is to determine whether the selected model structure reliably and adequately represents the hydrologic processes at the ungauged catchment of interest [28].

Rainfall-runoff models and hydrological model-independent methods have played a huge role in the regionalization of continuous stream flow [29]. Model parameters are used as a means of transferring hydrologic information from gauged to the ungauged basins, rather than a direct transfer of stream flow data through portioning methods [6]. In a process-based water quality model, such values may be numerous, and the problem of equifinality may arise, *i.e.*, many model setups may yield similar model performance [30]. Due to heterogeneity, it is always very difficult to link all model parameters to the correct watershed characteristics [31]. The success of transferring hydrologic information between watersheds could be influenced by the spatial proximity and physical similarity between the donor (gauged) and recipient (ungauged) watersheds [32]. In other cases, regression equations that incorporate different gauges in a watershed with similar hydrologic characteristics are useful methods for extrapolating calibration parameters to ungauged sites [14] [29].

The SWAT (Soil and Water Assessment Tool) is an open-source distributed model [33] [34] that has a large and growing application in the hydrological characterizing of catchments [6]. Regarding previous studies, the tool has shown strength in discharge estimation in mountainous catchments [1] [35]. The model has successfully been used to estimate flow rates on a wide scale and in various hydrological regions. It was applied to evaluate the uncertainty and regionalization of hydrological information in numerous catchments [8] [9] [36] [37]. It is important to note that most of the above research involved the use of numerous existing gauges within a given watershed or pre-existing hydrologic regression equations.

The review report (the Decade of Prediction in the Ungauged Basins initiative (PUB 2003-2013)) indicates that the inability to make reliable predictions in ungauged watersheds will continue to impede sustainable water resources man-

agement and the development of effective flood and drought mitigation strategies, particularly in developing countries [31]. In the context of one or two gauges in a catchment with numerous river basins, the question is, "is calibrating a hydrological model using a single gauge's data points an optimal strategy to estimate flows in other ungauged regions of the catchment?" Thus, this study endeavors to share a framework that employs a blend of spatial proximity (direct transfer of calibrated model parameter) and physical similarity (discharge ratio-scaling of various simulated scenarios) approaches to achieve better model predictability at the ungauged site.

2. Materials and Methods

2.1. The Study Area

Isahaya Reservoir (with an area of 26 km^2 and 29 × 10^6 m^3 holding capacity) was constructed at the innermost part of Isahaya Bay (Ariake Sea, Kyushu Island in southern Japan—**Figure 1**) to prevent flooding disasters and to protect reclaimed farmlands [38]. In April 1997, the inner part of the bay was separated from the main sea by a dike 7 km long and 200 m wide. Construction of the dike enclosed 35 km^2 of Isahaya Bay's tidal flats, which is 2% of the total area of the Ariake Sea [39].

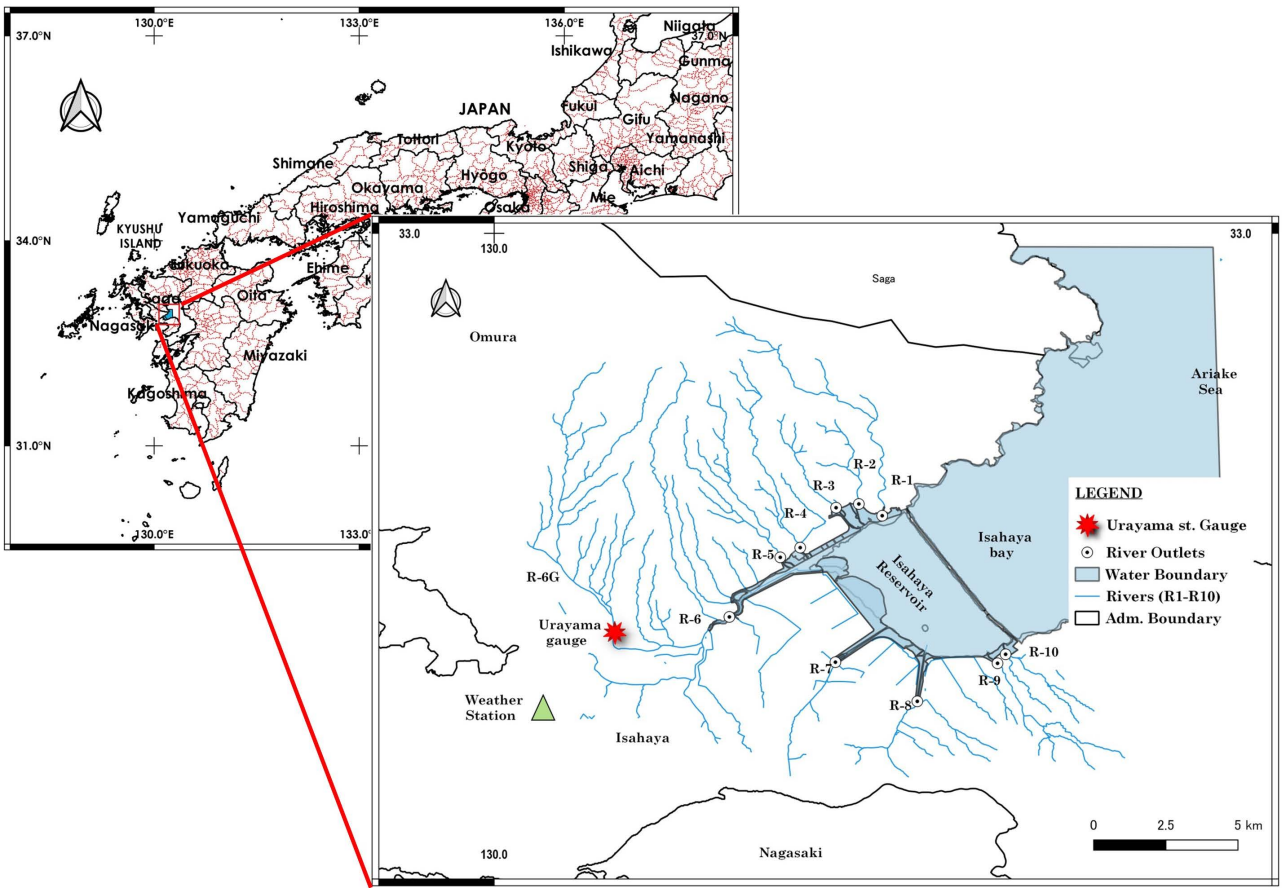

Figure 1. The location of Isahaya Reservoir Catchment.

Table 1 summarizes the entire Isahaya Reservoir watershed (area 248.67 km^2) with details of the ten river basins (211.34 km^2). The entire catchment is ungauged apart from a single gauge upstream of the Honmyo River (R6G) basin, covering an area of 37.336 km^2 with an average slope of 0.258 m/m. The 10 river basins are characterized by human interference with the course of the river for agricultural purposes, especially in the downstream sections. The climatic condition is temperate, with semi-humid, rainy summer seasons. Wet and high temperatures are experienced during the summer months, while dry and low temperatures prevail in the winter months. The average annual temperature in Isahaya is 16.3˚C. Over the course of the year, the temperature typically varies from 3˚C to 31˚C and is rarely below −1˚C or above 34˚C. On average, June is the wettest month with precipitation of about 350.0 mm and December is the driest month with total precipitation of about 65.0 mm. The region experiences annual total precipitation of 1800 - 2200 mm. Stream flow usually peaks in the middle of summer seasons because of heavy rainfall or typhoons. The information of interest for the behavior of the basin is therefore largely focused on the hydrographs of the summer season. Snow accumulation and ablation are rare occurrences due to low elevation in the Isahaya catchment. Thus, snow has a negligible effect on runoff variations in this watershed. It accounts for an insignificant portion of winter precipitation [40] [41].

2.2. Data Acquisition

Table 2 shows the available SWAT (Soil and Water Assessment Tool) model input datasets used in this research. 18 Intermittent flow rate data for each of the

Table 1. Details of Isahaya Reservoir Catchment.

River Basin	Area km^2	Avg Slope m/m	% Land cover						
			AGRR	RICE	RNGB	FRST	FRSE	FRSD	URBN
R1-Sakai	18.69	0.288	2.1	4.31	-	43.87	40.53	6.23	2.21
R2-Yue	6.85	0.185	10.18	21.67	2.87	26.03	30.43	21.67	6.47
R3-Tajima	5.13	0.242	2.92	14.64	-	49.75	27.11	1.16	2.3
R4-Oe	10.89	0.245	6.92	18.4	-	42.12	24.09	4.39	3.48
R5-Fukanomi	12.82	0.227	6.73	12.22	1.41	53.98	22.96	1.47	1.15
R6G-Honmyo	37.33	2.58	9.48	10.76	2.94	37.55	32.37	2	4.65
R7-Nitanda	12.69	0.195	16.22	39.78	4.24	4.74	24.95	-	8.36
R8-Ariake	24.95	0.14	24.14	38.99	2.92	4.46	19.09	-	9.01
R9-Yamada	11.94	0.197	11	11.64	3.27	34.25	34.01	2.47	3.04
R10-Tagawahara	5.93	0.177	12.12	24.14	-	21.21	31.8	-	8.61

R6G; Gauged River basin (upstream section of Honmyo River), AVG; Average slope, AGRR; Agricultural Land-Row Crops (mainly Vegetables-warm season), RICE; Rice farms, RNGB; Range-Brush, FRST; Forest-Mixed, FRSE; Forest-Evergreen, FRSD; Forest-Deciduous, URBN; Urban areas with high density.

Table 2. Model input dataset.

Data type	Scale	Source	Description/properties
Digital Elevation Map (DEM)-TIF	Resolution 10 m × 10 m	USGS Earth explorer	Elevation, slope, channel lengths
Soils-TIF	Japan 1:50,000	Japanese soil inventory	2017 Version
Land Use-TIF	10 m resolution	Jaxa, Japan	2018-2020 version
Weather Information-CSV	Daily Precipitation (mm), Max & Min Temperatures (˚C), Relative humidity (%), Wind speed (m/s) and Solar radiation (Mj/s^2)	Isahaya City, Omura (Nagasaki Airport) and Nagasaki Met. stations (Japan Meteorological Agency Website)	Up to date data with no gaps Jan. 2013-Jul. 2020. D
Honmyo River Discharge (Upstream at Urayama St.)	Hourly Water level data with H-Q equation ($Q = A(H + B)^2$) for specific periods of time. Where A and B are constants	Ministry of Land, infrastructure, transport, and tourism-water resource department	Gauged data from Jan. 2016-Jul. 2021
River Discharge for the ungauged basins	18 mean flow rate data (m^3/s) at each river discharge point	Use of electromagnetic current meter and cross section at discharge point	Measured between March-July 2021

NOTE: Crop management within Isahaya region was informed from Kyushu region and Nagasaki Prefectural reports and related research work. Such information encompassed, Land preparation period, types of crops, fertilization regimes, crop/land management operations, Harvesting and post-harvest operations (Fumikazu & Erdinc, 2013).

9 rivers were measured for 4 months. At the discharge point of each river, several depths and points across the river were recorded in meters to obtain the cross-sectional area and flow (velocity) captured in m/s. The measured cross-section area and the flow velocity were used to compute the daily flow rate at the discharge points in m^3/s. Multiple measurements were made at each discharge point within the observational day and averaged to determine the daily mean flow rate (expounded in section 2.5).

2.3. Hydrological Characteristics of R6G Basin (Urayama Station Upstream)

The gauged part of the R6G basin was simulated using the above data set. The model SWAT was calibrated using gauge height data from the Urayama gauging station for the years (08/2016-07/2018). A sensitivity analysis was performed to determine the influence of each parameter included in the calibration on the flow rate. Model performance was then validated for 08/2018-07/2020 and 08/2019-07/2021. SWAT-CUP (a Calibration Uncertainty Program for SWAT based on the Sequential Uncertainty Conformity Algorithm-SUFI2) was used for calibration and validation and to determine the sensitivity of the calibration parameters. SUFI-2 is a semi-automatic optimization procedure that uses the Latin hypercube sampling method and is a highly efficient sampling method for obtaining optimal results. It can handle a large number of parameters, perform calibration on multiple measurement stations, and allows the use of different objective functions [42].

2.4. Extrapolation of Hydrological Characteristics from the Gauged R6G River Basin to the Ungauged River

Weather data from the three stations (Nagasaki, Omura, and Mt. Unzen) in the Nagasaki region were compared to determine seasonal variations in the region. Due to the high correlation results, the nearest weather information (Omura Meteorological Station) was adopted for the 10 streams. The 10 streams run downstream from the mountainous region east, south, and west of the reservoir with similar elevations at the discharge points (part of the Ariake sea). Based on the proportional similarity in soil characteristics, land uses, and geological history, the underground water flow characteristics, unless determined, were assumed to be like the gauged river throughout the study area.

The observed daily discharge data at the Urayama gauging-station (R6G) were denoted as Q_G (m^3/s) and the resulting simulated flow rate of the gauged river was denoted as Q_{Sim} (m^3/s). Since there was no continuous data at the ungauged site, the parameters of the gauged site were integrated into the model building to obtain Q_{sim} (m^3/s). Due to the inexistence of a second gauge in the watershed, the use of methods such as global averaging or regression [43] to estimate discharge at the ungauged site was untenable. Considering the proximity and similarity between donor and recipient, the R6G parameters were globalized. Two methods were used to globalize (DG) hydrologic parameters within the watershed. First (DG), assuming similar groundwater characteristics and comparable soil hydrologic groups, the parameters were adopted from R6G (donor). For the second criterion (DG-1 & DG-2), an attempt was made to modify the groundwater lag value by considering the area of the watershed and/or the slope factor.

To determine the criterion for transplanting hydrologic flow signatures from the gauged site to the ungauged basin, different scenarios were tested separately with respect to land use/land cover and soil types to determine their influence on the flow rate. In the 9 streams, two or three soil types covering a reasonable area did not influence the changes in discharge rate. In most cases, altering the soil's characteristics didn't result in a significant change in flow signals. Changes in land use had a significant influence on the continuous discharge of the 10 river basins (including the gauged stream). Sensitivity analysis is critical because the new framework is based on the proportional influence of such factors on the transplantation of flow signals from the donor basin to the recipient basin.

The parameters from R6G were adopted by DG for model build-up at the 9-ungauged sites as baseline information for the watershed. Considering three land use scenarios and holding other factors constant, a continuous runoff was simulated independently for each of the following scenarios (the superscript indicates the gauged site (donor) and the lowercase indicates the (ungauged) river basin):

a) Q_F and Q_f (m^3/s)—The river basin was simulated with respective forests (deciduous, evergreen, and mixed) and high-density urban land use, taking into account the new hydrologic features. The agricultural land, *i.e.*, rice, row crops (mainly warm-season vegetables), and Range bush (including citrus orchards),

was classified as wasteland (barren land).

b) Q_H and Q_h (m^3/s)—The river basin was simulated with respect to human activities (agricultural land under crops in rows, rice, and citrus plantations) and Urban high-density land use. The land under the forests was set as barren.

c) Q_B and Q_b (m^3/s)—The river basin was simulated with barren land uses in a. and b., while the corresponding areas were maintained under high-density urban land uses.

Example R8: AGRR-24.4%, RICE 38.99% RNGB 2.92%, FRST 4.46%, FRSE 19.09% and URBN 9.00% of 24.95 km^2.

a) Q_f (m^3/s): The FRST 4.46% and FRSE 19.09% of 24.95 km^2 was maintained while AGRR-24.4%, Rice 38.99% and RNGB 2.92%, is set to barren. The URBN 9.00% of 24.95 km^2, is also maintained.

b) Q_h (m^3/s): TheAGRR-24.4%, RICE 38.99% RNGB 2.92% of 24.95 km^2, was maintained while the FRST 4.46% and FRSE 19.09%, is set to barren. The URBN 9.00% of 24.95 km^2, is also maintained.

c) Q_b (m^3/s): The AGRR-24.4%, RICE 38.99% RNGB 2.92%, FRST 4.46%, FRSE 19.09% was set as barren. The URBN 9.00% of 24.95 km^2, is also maintained.

The above scenarios were simulated independently for each river (R.No.), and the resulting continuous discharge was stored in a spreadsheet for the period 08/2016-07/2020 against the results of the calibrated river R6G. To map the dynamics of the discharge recorded by the gauging station to the ungauged basin and to use the influence of land use on the discharge characteristics (gauged and ungauged basins), the following correction factor was used. At time *t*, the relationship between the observed mean daily flow rate Q_G and the calculated mean daily discharge Q_T for the gauged basin was defined as:

$$C = \frac{Q_G}{Q_T} \tag{1}$$

Following that, the daily runoff at the discharge point is substantially influenced by the forest and by human activities. Taking account of the urban region as a fraction of the discharge obtained in the third scenario (Q_B or Q_b), the total discharge at time T ($Q_{(T)}$) for R6G and t ($Q_{(t)}$) for the ungauged rivers was defined as:

$$Q_{(T)} = Q_F + Q_H - \left(1 - \kappa_A\right) Q_B \tag{2a}$$

$$Q_{(t)} = Q_f + Q_h - \left(1 - \kappa_a\right) Q_b \tag{2b}$$

where: κ is a fraction of urban area with high density land use and/or fraction within each scenario if changed to barren.

Considering the differences in flow rate at each time t-step, a correction factor ratio C_f was determined as follows depending on the influence of the land uses within the donor and recipient river basins.

$$C_f = C - \left(\frac{\left|Q_H - Q_h\right|}{3Q_H} + \frac{\left|Q_F - Q_f\right|}{3Q_F} - \left(\kappa_a - \kappa_A\right) \frac{\left|Q_B - Q_b\right|}{3Q_B} \right) \left(\frac{1}{C} - 1 \right) \tag{3}$$

where: C_f is the correction factor ratio at time t and k_A and k_a are the fraction of the urban high density land use of the gauged and ungauged river basins, respectively.

The estimated daily flow at the ungauged discharge site was determined as follows to account for hydrologic differences in flow signatures within the donor and recipient when transferring flow characteristics from the observed data.

$$Q_{ung(t)} = C_f \times Q_{(t)} \tag{4}$$

A comparison was made between the discharge predicted by the new framework method (N.F.), *i.e.*, Q_{ung} ($m^3 \cdot s^{-1}$) and the 18 observed intermittent discharges (obtained between March 2021 and July 2021) to determine the performance of the applied method used at a given discharge point for each of the 9 river basins.

2.5. Stream Flow Measurement with the KENEK VPT-200-24

Discharge estimates were obtained by measuring river flow with the Kenek VPT-200-24 flow meter and cross-sectional area (using a depth staff and tape measure). The Kenek VPT-200-24 flow meter is an ideal instrument for measuring flow in rivers and lakes or reservoirs with a wide range of water quality (tap water quality to industrial wastewater).

The flow rate (Q_m in m^3/s) was calculated from the velocity profile using the mean-section method, which uses the depth d_n (m) at a series of two verticals in a cross-section and the distance between the verticals b_n (m) to determine the cross-sectional area for each subsection. The depth-averaged flow velocity $\bar{v}_n$ ($m^2 \cdot s^{-1}$) in each vertical was estimated by measuring the velocities at several points along the n^{th} vertical. Cross-sectional discharges are computed as the product of the segment area and the depth-averaged velocity. Total discharge was computed as a summation of sectional discharges as defined in Equation (5) and Figure 2.

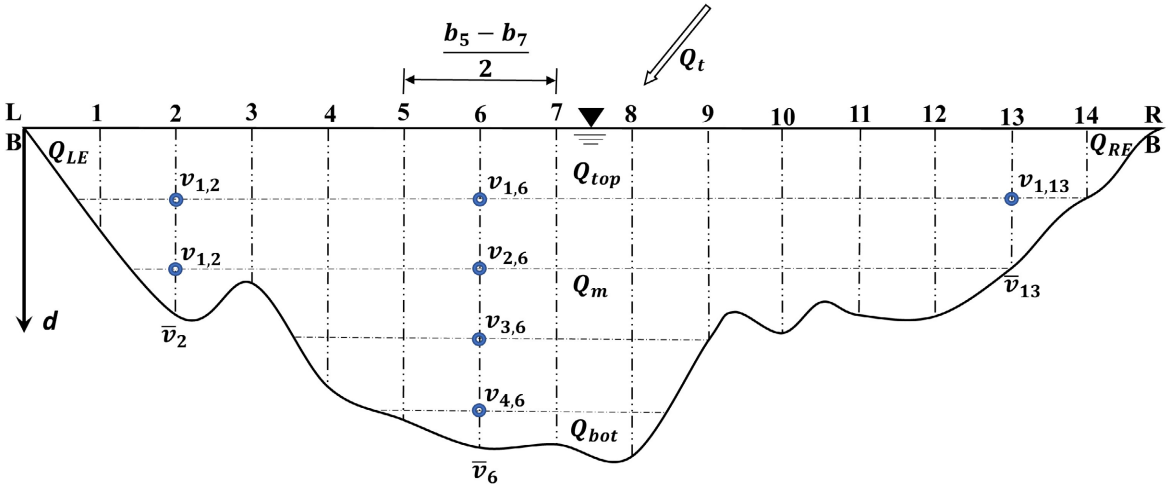

Figure 2. Sample of stream flow measurements (discharge point-R8) using VPT2-200-24.

$$Q_m = \overline{v}_1 \times d_1 \times \left(\frac{b_2 - b_1}{2}\right) + \sum_{n=2}^{13}\left(\overline{v}_n \times d_n \times \left(\frac{b_{n+1} - b_{n-1}}{2}\right)\right) + \overline{v}_{14} \times d_{14} \times \left(\frac{b_{14} - b_{13}}{2}\right) \quad (5)$$

where for example;

R8, 13 subsections were considered as represented in Figure 2.

Assuming the edges toward the river banks were approximately triangular, the edge coefficient of 0.3535 was adopted [44]. This applied to all other 8 river channels except for river R9 channel. Thus, at the edges, discharge was defined as:

$$\text{QLE} = 0.3535 b_1 d_1 \overline{v}_1 \quad (6)$$

and

$$\text{QRE} = 0.3535\left(b_{RB} - b_{14}\right) d_{14} \overline{v}_{14} \quad (7)$$

The total discharge Q_T was then defined as:

$$Q_T = \text{QLE} + Q_m + \text{QRE} \quad (8)$$

At the discharge point of the river, R9 is a well-defined rectangular weir. The discharge was therefore determined to be equal to Q_m with the numbering of verticals running from the end to the end of the riverbank (1, 2, 3 … n^{th}).

2.6. Definition of the Objective Functions

To calibrate the model and determine how optimally the simulation reproduces the observed information, the objective functions: NSE, R^2, and bR^2 objective functions were considered.

1) Nash-Sutcliffe model efficiency coefficient (NSE)

The NSE was used to evaluate the predictive power of the model that replicates the hydrologic functions in the studied watersheds. It was defined as:

$$\text{NSE} = 1 - \frac{\sum_{t=1}^{T}\left(Q_m^t - Q_0^t\right)^2}{\sum_{t=1}^{T}\left(Q_o^t - \overline{Q}_0\right)^2} \quad (9)$$

where: $\overline{Q}_0$ is the mean of observed discharge, Q_m^t is modeled discharge, and Q_0^t is observed discharge at time t.

NSE range is $-\infty \geq 1$; Values of NSE ≥ 0.5 were satisfactory.

2) The Pearson Coefficient of Correlation, R^2

R^2 is a measure, of how well-observed results are replicated by the model simulation based on the proportion of total variation in the results. The Coefficient of Correlation R^2 was defined as:

$$R^2 = \frac{\left[\sum_i\left(Q_{m,i} - \overline{Q}_m\right)\left(Q_{s,i} - \overline{Q}_s\right)\right]^2}{\sum_i\left(Q_{m,i} - \overline{Q}_m\right)^2 \sum_i\left(Q_{s,i} - \overline{Q}_s\right)^2} \quad (10)$$

where: Q *is* a variable (discharge), and m and s stand for measured and simu-

lated, i is the i^{th} measured or simulated data.

R^2 range is 0 ≥ 1; Values of R^2 ≥ 0.5 were satisfactory.

3) Modified coefficient of determination, bR^2

The coefficient of determination R^2 is multiplied by the slope of the regression line b between the simulation results and the measured data. This function takes into account both the discrepancy in the magnitude of two signals (depicted by b) and their dynamics (depicted by R^2) [45].

$$\text{Maximize}: \varnothing = \begin{cases} |b| R^2 & \text{if } |b| \le 1 \\ |b|^{-1} R^2 & \text{if } |b| > 1 \end{cases} \tag{11}$$

bR^2 range is 0 ≥ 1;Values of bR^2 ≥ 0.5 were satisfactory.

Regarding to the merits and demerits associated with each one of the three objective functions [32] [45] [46], the three were used to complement each other's shortcomings and evaluate the precision of the model prediction.

3. Results and Discussion

3.1. Calibration and Validation of the Gauged R6-G River Basin

SWAT-CUP SUF2 was used to calibrate and validate of the model output against the available gauged data. The performance of the model was recorded in Table 3 for the calibration periods (1 and 2). The resulting hydrograph (Figure 3) showed that the peak signatures, decline, and base flows were accurate compared to the observed data at the Urayama gauging station.

As recorded in Table 3, the model performance improved remarkably during validation period 1 & 2, depicting the flow rate and the trend at the gauge station (R6G). Although the number of daily flow rates covered within the 95PPU band decreased, the shrink in the band by half and the increase in NSE and R^2 indicated the precision. Despite the difference in peak flow in the second validation, the model performed adequately. The high precision of these results could imply

Table 3. Model performance during calibration and validation for the gauged R6G basin.

Objective function	Calibration 08/2016-07/2018	Validation-1 08/2018-07/2020	Validation-2 08/2019-07/2021
p-factor	0.91	0.83	0.85
r-factor	0.67	0.32	0.30
NSE	**0.91**	**0.95**	**0.93**
R^2	0.91	0.95	0.94
bR^2	0.8821	0.8804	0.8865
Mean simulated. (Mean observed)	2.27 (2.10)	2.48 (2.45)	3.40 (3.52)
Std Dev.-simulation (Std Dev.-observed)	4.08 (4.02)	7.31 (7.70)	9.78 (10.28)

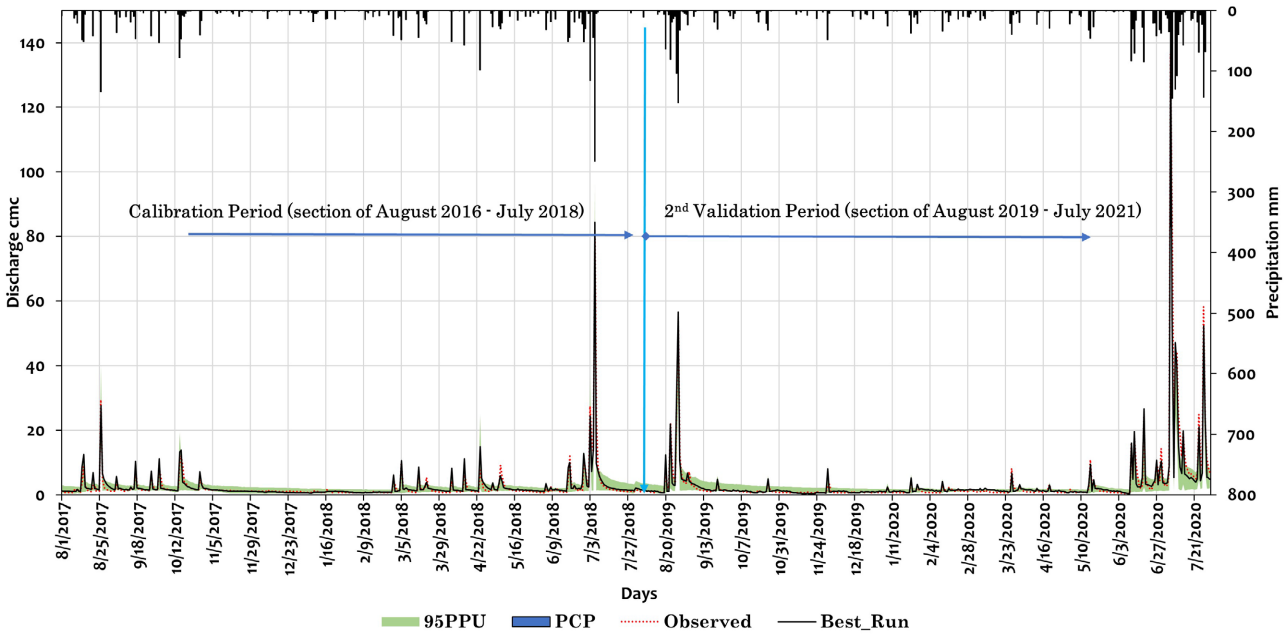

Figure 3. The flow characteristics of R6G basin during calibration and 2nd validation period.

that: The model choice was appropriate for this mountainous river basin and that the input data, the crop schedule, and the weather data were true representatives of the region.

As discussed by various articles, this underscores the importance of model choice and correction of data from measuring instruments or other related accrued errors before use in modeling [47] [48]. Successful use of the distributed model to simulate river discharge depends on the characteristics of the input data, observational data for calibration, and the selection of an appropriate model for the study region. This ensures the robustness of the model results and adequate simulation of the flow responses of a watershed [46]. The choice of a model and the quality of the data used are reflected in a successful simulation, *i.e.*, parameter values within a reasonable range and without overparameterization. This ensures proper calibration and validation of model results against a specific measured hydrologic feature [49]. The R6G river basin was adequately calibrated for 08/2016-07/2018 observed data and validated against a new set of data 08/2018-07/2020 and 08/2019-07/2020, as captured in **Table 3**, and partly in **Figure 3**, above.

During calibration, 9 parameters were used as recorded in **Table 4**. The river routing parameters were the most sensitive in the R6G basin. The sensitivity of the parameters during calibration follows the list in **Table 4**, column 1, denoted by a rank number. Groundwater delay (days) had the least influence, while the base flow factor for bank storage had the highest influence on the flow rate response during calibration of the SWAT model. The best simulation was realized when the model parameters were fitted at the values in **Table 4**, column 4. The mean daily flow for the basin post-calibration model was 2.48 m^3/s with the maximum

Table 4. The parameters utilized in the calibration of the SWAT model for the R6G basin.

Sensitivity Rank	Calibration Parameters	Description of the parameters	Fitted Value	Min. value	Max. value
1	V__ALPHA_BNK.rte	Base flow alpha factor for bank storage.	0.4035	0.0	0.5
2	V__CH_N2.rte	Manning's "n" value for the main channel.	0.0183	0.0	0.3
3	V__CH_K2.rte	Effective hydraulic conductivity in main channel alluvium.	148.325	5.0	200
4	V__ALPHA_BF.gw	Baseflow alpha factor (days).	0.06481	0.01	0.3
5	R__SOL_AWC().sol	Available water capacity of the soil layer.	0.2459	−0.2	0.5
6	V__SHALLST.gw	Initial depth of water in the shallow aquifer (mm).	798.5	500	2000
7	R__SOL_K().sol	Saturated hydraulic conductivity.	1.1831	−0.5	2.5
8	R__CN2.mgt	SCS runoff curve number.	−0.1244	−0.2	0.2
9	V__GW_DELAY.gw	Groundwater delay (days).	37.758	2.0	40

peak during the summer period (June-July) and lowest flow in the winter period (December-January) compared to 2.45 m^3/s as observed.

3.2. Transplant of Hydrological Flow Characteristics from Gauged to Ungauged Basins

The parameters altered in calibration and validation of R6G provided basic hydrological characteristics of the Isahaya catchment (since exists only a single gauge in the whole catchment). The assumption of approximate homogeneity in the cases of DG makes the method very simplistic. Adopting all the parameters' values (DG) as attained in R6G, the resultant hydrograph correlated reasonably with the observed intermitted dataset but overestimated or underestimate the mean daily flow rate. Modifying some of the globalized parameter(s) using an implicit equation could improve the accuracy of estimated discharge at an ungauged site. Using such implicit equations (Equation (12) or Equation (13)) as DG-1 and DG-2 below to alter the groundwater delay only improved precision in depicting the trends for R1, R2, R5, and R7 as compared to the observed dataset.

$$GW_{DR.No} = GW_{DR6G}\left[\frac{A_{R.No}}{A_{R6G}}\right]^{SLP_{R6G}/SLP_{R.No}} \tag{12}$$

or

$$GW\_D_{R.No} = GW\_D_{R6G}\left[\frac{A_{R.No}}{A_{R6G}}\right] \tag{13}$$

where; GW_D is ground water delay, R.No is river number (1, 2, 3…), A is the watershed area, SLP is the avarage slope.

Figure 4 and Table 5 are the results of DG, DG-1 & DG-2 attempts to characterize continuous flow at the ungauged site. The overestimation or underestimation of the flow rate and the absence of crests during large rainfall events

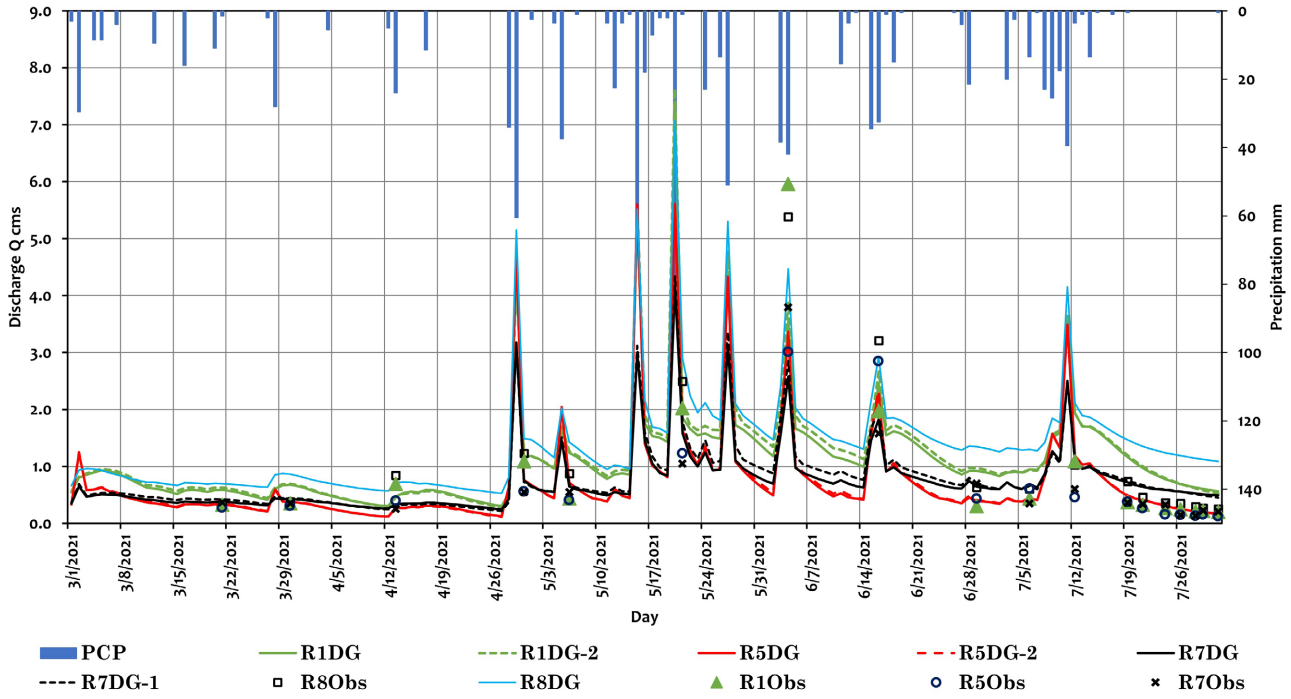

Figure 4. The flow characteristics at ungauged R1, R5, R7, and R8 using DG against observed data.

Table 5. Evaluation of flow characteristics at the ungauged site using direct globalization.

DG	OBJ.FXN	R1	R2	R3	R4	R5	R6	R7	R8	R9	R10
DG	NSE	0.6829	0.6380	0.7971	0.8014	0.8937	GAUGED	0.7576	0.7030	0.8210	0.7961
	R^2	0.8286	0.8880	0.8556	0.8453	0.9086		0.8592	0.9162	0.9589	0.8711
	bR^2	0.4387	0.4139	0.7754	0.6532	0.8455		0.5445	0.6255	0.8638	0.7952
DG-1	NSE	0.6950	0.7330	0.7789	0.7887	0.8924		0.7776	0.6086	0.7797	0.6953
	R^2	0.8325	0.8891	0.8525	0.8338	0.9126		0.8653	0.8664	0.9578	0.8535
	bR^2	0.4664	0.4613	0.8093	0.7410	0.8750		0.6252	0.7094	0.9534	0.7995
DG-2	NSE	0.7165	0.7303	0.7809	0.7906	0.8930		0.7733	0.6904	0.7871	0.7120
	R^2	0.8429	0.8968	0.8541	0.8356	0.9130		0.8659	0.9205	0.9618	0.8658
	bR^2	0.4998	0.4594	0.8094	0.7399	0.8729		0.6113	0.6683	0.9424	0.8240

were some of the misrepresentations of the hydrography at the ungauged site using the methods DG, DG-1 & DG-2. Although the above methods represent the trend at ungauged sites, they are abstract because river basins have some heterogeneity despite their proximity to the donor. Changes in calibration parameters are relative to other parameters at a given site despite similarity and proximity. This was evident in the way different river basins responded to changes in groundwater delay value as per Equation (12) and Equation (13). In rare cases, a changing a single parameter can lead to an optimal simulation. In the case of a single gauging station, it was not possible to change parameters relative to other parameters due to scanty hydrological information about the wa-

tershed. Due to these uncertainties, the method described above is not reliable and cannot be applied to other sites with similar hydrological characteristics.

Using DG as baseline information that can be assigned to the watershed, flow characteristics were estimated at an ungauged station for each of the 9 river basins according to the new framework (N.F) described in Section 2.4. Precision and reproducibility were evaluated, and the baseline information from DG was incorporated into the modeling prior to applying the N.F. Although DG-1 and DG-2 showed better trend precision for R1, R2, R5, and R7, the resulting N.F hydrograph was close to the DG when used in model building for the N.F. To determine whether the N.F. estimates reflect the actual flow rate at the ungauged discharge point, the characteristics of the resulting hydrographs were statistically compared with the 18 intermittently observed flow records.

The continuous flow rate mapped from the gauged stream to the ungauged site by the N.F showed representative estimation as compared to the use of the DG method (**Figures 5(a)-(d)**). The N.F exhibited robustness in estimating base flow and peaks as a response to reasonable precipitation events. The problem of overestimating base flow or missing the peaks even with sufficient precipitation events was correctly represented by the N.F. method of transplanting signatures relative to the donor. This phenomenon was much pronounced in R1 & R8, R3 & R10, R5, and R9 as represented in **Figures 5(a)-(d)**, respectively. DG is associated with certain levels of uncertainty, depending on the proximity and similarity between the recipient and the donor watershed [50]. Maintaining such rigidity of flows would adversely affect the physical and biochemical analysis of additional watersheds. Non-responsiveness of flow signals could be due to the assumption that the physical catchment attributes of the gauged basin adequately mirror those of the recipient, thus proportionately influencing changes in flow rate.

The N.F., as applied to the 9-ungauged sites, proved suitable for characterizing continuous flow rate in a data-scarce watershed (summarized in **Table 6**). Although the accuracy of the new framework was lowest for R1 and R2, the result was a reasonable estimate compared to the observed flux data (**Figure 5(a)** and **Figure 5(b)**). In the donor, R-6G, the watershed area is 71% forest and 21% farmlands, while the R1 basin is 90% forest and only 7% of the land is used for farming activities. The R1 basin, too, has the highest slope in the whole catchment. These factors and proximity to the donor basin may have influenced the results of DG and N.F. compared to estimates at discharge points on other rivers. However, the net effect was more pronounced with the DG method than with the N.F. method. The N.F. method's prediction best depicted the trend and response of flow to precipitation events. The results are reliable for further analysis of the watershed. The R2 difference in land use coupled with a lower slope as compared to the donor might have influenced the transplant of flow signals.

The R3 river basin is relatively small (about the same size as R1 and R2), but the similarity in slope and proportion of land use to the donor catchment can be

related to the high accuracy of the N.F. (Table 6 and Figure 5(b)). The R8 basin has the lowest gradient and is the least forested compared to the other 9 river basins draining into the Isahaya Reservoir. The land use characteristics are quite different from the gauged river basin (R6G), where more than 65% of the land is used for agriculture (for the other 7 rivers, more than 70% of the land is covered by forests). These differences didn't influence the transplanting of flow signals from the donor. The sharp decline in the observed intermittent flow rate towards

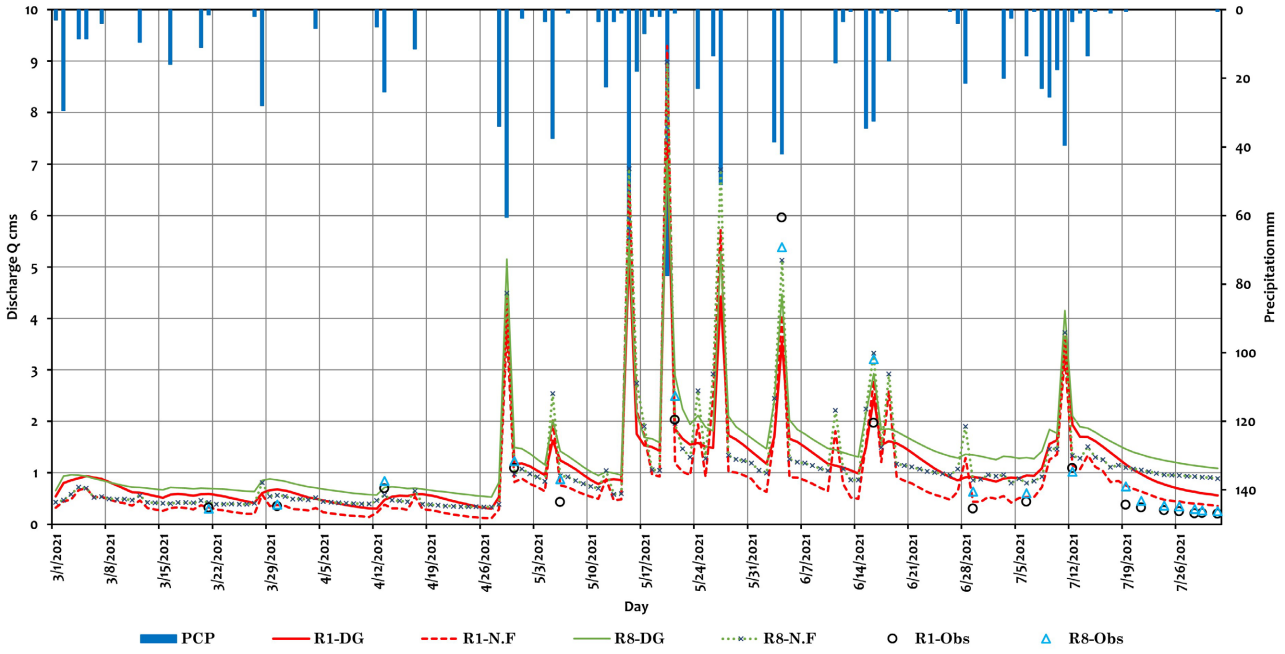

(a)

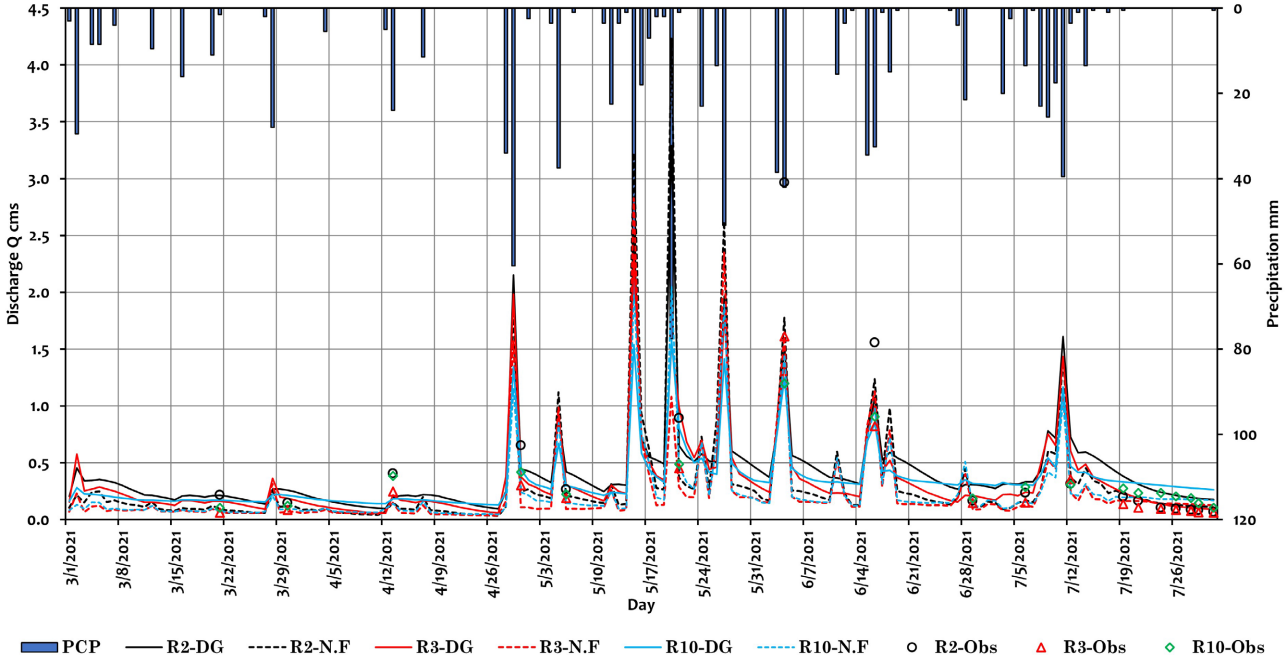

(b)

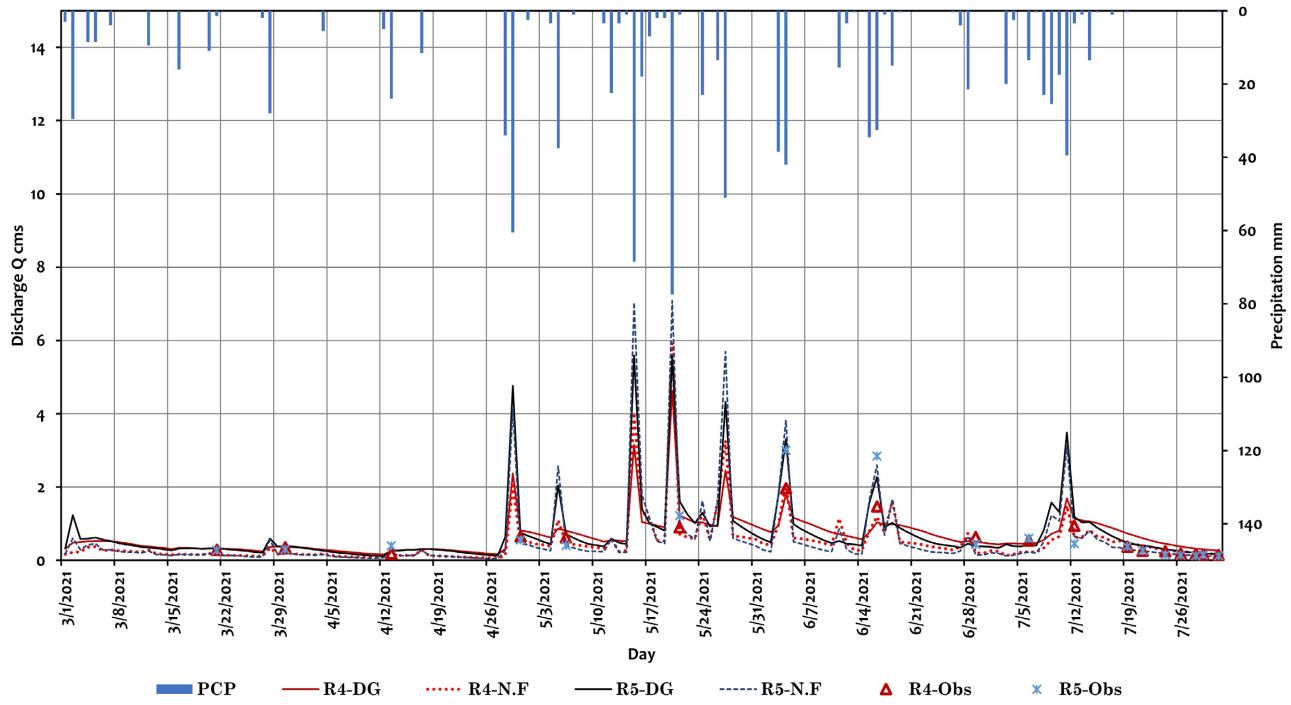

(c)

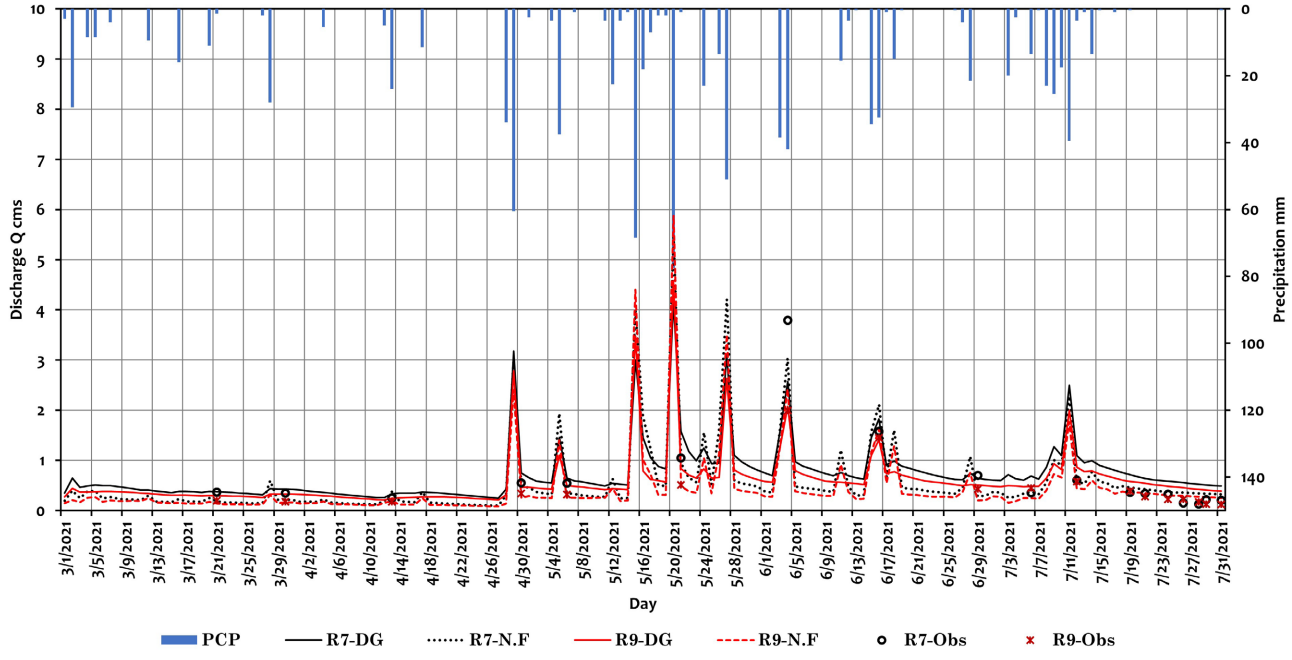

(d)

Figure 5. Ungauged River basins' flow characteristics using DG, and N.F in comparison with intermittent observed data. (a) R1 and R8 basins' flow characteristics using DG & N.F. in comparison with intermittent observed data; (b) R2, R3, and R10 basins' flow characteristics using DG & N.F in comparison with intermittent observed data; (c) R4 and R5 basins' flow characteristics using DG & N.F in comparison with intermittent observed data; (d) R7 and R9 basins' flow characteristics using DG & N.F in comparison with intermittent observed data.

the end of July was of concern and may indicate that much water was diverted to rice farms due to reduced rainfall. From the results of the 9 river basins shown in

Table 6. Summary of the N.F precision as applied at the ungauged basins to estimate flow.

River Basin	W. Area	Slope	D-flow	%FRST	%HUM.A	Objective Functions		
	Km^2	m/m	m^3/s			NSE	R^2	bR^2
R-1	18.69	0.29	0.868	90.63	7.01	0.8253	0.8776	0.5824
R-2	6.852	0.19	0.346	58.66	34.5	0.7694	0.9403	0.5626
R-3	5.129	0.24	0.242	78.2	18.32	0.9128	0.9251	0.8971
R-4	10.89	0.25	0.551	70.6	25.78	0.8426	0.8786	0.7998
R-5	12.82	0.23	0.557	78.41	20.36	0.9097	0.9437	0.8457
R-6G	37.33	0.26	2.441	71.92	23.18	Donor gauge		
R-7	12.69	0.2	0.614	30.07	60.24	0.8965	0.9053	0.7408
R-8	24.95	0.14	1.016	23.55	66.05	0.8945	0.9344	0.7802
R-9	11.94	0.2	0.498	70.73	25.91	0.9019	0.9523	0.8160
R-10	5.93	0.18	0.28	53.23	37.23	0.8457	0.9344	0.7819

W. Area: Watershed Area, D-flow: Daily Mean Flowrate, %FRST & %HUM.A: Percent Watershed area under Forests and Human activities (mainly farmlands).

Table 6, it is evident that the N.F provides reasonable and reliable results in transferring the hydrologic continuous discharge characteristics of the gauged donor basin to the ungauged recipient basin in the ungauged watershed.

Proportional scaling utilizing land use influence on discharge between the two basins showed adequate predictability and reduction in the loss of flow signatures in the event of direct globalization. Thus, the N.F. could be used in transferring runoff characteristics from gauged to ungauged river basins in a watershed with scarce flow data or without other hydrologic information. Despite the difference in size, slope, or land use, the method showed adequate flow response to weather and catchment characteristics at the ungauged site. The N.F. provides an alternative method for reasonably estimating discharge at an ungauged location when the number of gauges is limited, and other methods are inapplicable or ineffective.

The attributes used in the regionalization of flow characteristics in the pursuit of estimating the flow rate at the ungauged site include proximity, the catchment area, elevation, the slope of the basin or channels, land use, and weather conditions [29] [51]. In the Isahaya Reservoir watershed, area, slope, and land use are important aspects that affect the flow regime and influence the choice of method that can be used to transplant flow characteristics. The problem of data unavailability at the onset of this study raised the question; of what approaches could be adequate to estimate the flow rate at the ungauged basins with a single gauging station [52].

Using only a single gauge and several observation data, the N.F could be used to estimate flow characteristics of the ungauged basin. Where the direct parameter transfer method is impractical (e.g., lack of averaged watershed parameter

values or regression formula relating to hydrological characteristics within or outside the watershed), the N.F would aid in refining the estimates by accounting for differences or similarities with the donor basin [29]. When a rainfall-runoff model is to be selected, the model efficiency and applicability are some of the vital factors that a researcher needs to consider in the optimization of flow estimates in such a catchment with limited data [16] [53] [54] [55]. Selecting parameters for calibration or optimization needs to be considered, as well as the inclusion of associated uncertainties [56] [57] [58]. Due to proximity and similarity within the river basins, DG yielded a fair trend of flow rate estimates at the ungauged site but was inconsistent in determining the actual flow rate with changes in weather. The N.F. was able to refine the results of DG and provide an adequate estimate of discharge at the ungauged site.

3.3. The Uncertainties

3.3.1. The Uncertainties Inherent in the Hydrological Modeling

In SUFI-2, the parameter uncertainty is determined by all the input and output sources of uncertainties. These include the uncertainty in the input rainfall data, the land use and soil type, parameters, and observed data. During simulation, uncertainty is quantified by the 95% prediction uncertainty (95PPU) which is referred to as the p-factor. The 95PPU was calculated at the 2.5% and 97.5% levels of the cumulative distribution function of the output variable obtained by Latin hypercube sampling. The best calibration and parameter uncertainty is measured based on its closeness to the p-factor of 100% (the observations bracketed by the prediction uncertainty) and the r-factor of 1 (size of the uncertainty band). When the two factors are within a satisfactory range of values, a uniform distribution in the parameter hypercube is explained by the following parameter distribution. The goodness fit in SUFI-2 was quantified by the coefficient of Nash-Sutcliff model Efficiency (NSE) and Pearson correlation coefficient (R^2) between the observation data and the best simulation [36] [56].

Figure 6 shows a 95% prediction interval (dotted band) that indicates a 95% confidence interval for predicting a given day's mean flow rate of a specific river using the N.F model. The prediction interval is wider than the confidence intervals (grey band) because predicting the flow of the ungauged river on a given day by transplanting the hydrologic characteristics of a gauged stream has greater uncertainty than predicted based on the mean flow, which is proportional to the mapped/transplanted annual flow characteristics.

3.3.2. The Uncertainty in Discharge Measurement

The measurement process and use of data reduction equations provide the basis needed for conducting the uncertainty analysis. The analysis is vital in deducing the confidence in discharge determined for other institutions/researchers that would base their analysis on the already conducted research. The following are the computed uncertainties involved in the flow measurement at each discharge point (**Table 7**).

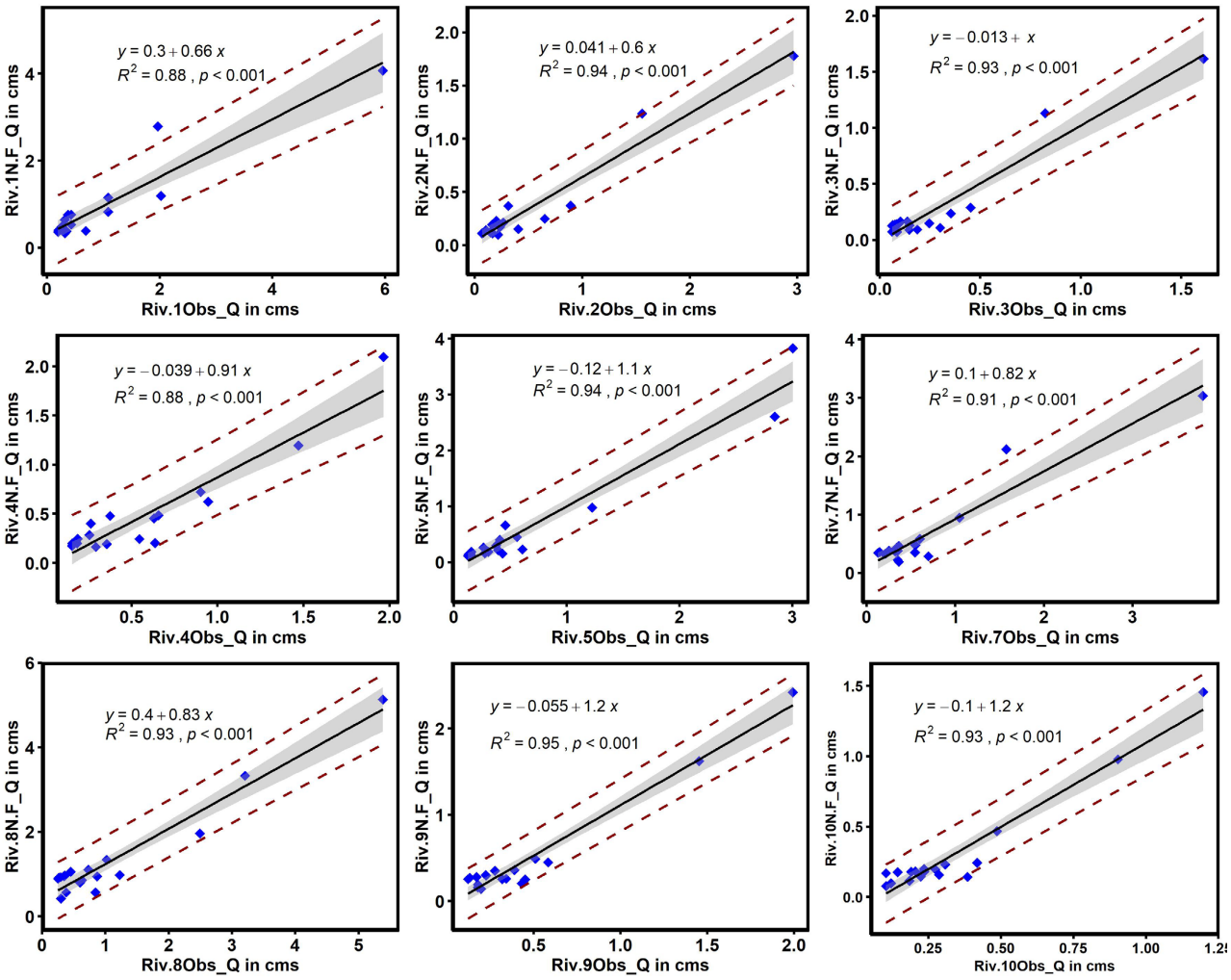

Figure 6. Regression plots showing prediction uncertainty of the flow rate (Q m^3/s) transplanted by the N.F in comparison to the observed intermitted datasets.

Table 7.[1] Computed uncertainty for the discharge measurement at each site.

River	R1	R2	R3	R4	R5	R7	R8	R9	R10
$U(Q_i)$	0.0336	0.0145	0.0124	0.0140	0.0380	0.0412	0.0624	0.0079	0.0087
Q_{Estimate}	0.8514	0.3113	0.2312	0.4769	0.5224	0.6095	0.9528	0.4554	0.2670
$\%\bar{Q}_{\text{estimate}}$	3.95	4.65	5.04	2.93	7.27	6.75	6.55	1.74	3.25

The low uncertainties at R9 (Table 7) are due to a triangular weir at the measurement site, implying a high probability of making similar measurements by different users. In all rivers, wading staff and ±2%/FS contributed significantly to the uncertainties. The uncertainties mentioned may have arisen during actual measurements at the discharge point. Other uncertainties, such as changes in flow outside the observation period, were not quantified. Such uncertainties should be considered when using the data or information from this work for

[1]**Appendix 2.** Calculation of the uncertainty in flow measurement.

further studies or analyses.

4. Conclusions

Natural systems in a watershed, such as rainfall-runoff processes, are complex, dynamic, nonlinear, and governed by multiple interrelated physicochemical components. Therefore, the successful use of simulations to describe the flow regime in a river basin requires the proper choice of a model, high-quality inputs, and observational data. The uncertainties associated with modeling such complex processes affect the reliability of the prediction of runoff at gauged and ungauged sites. Therefore, measured data are required for such models to force multiple variables to represent the process in the watershed and to ensure consistent and reasonable prediction of the stream flow. The unavailability of such data in many watersheds has been and continues to be an obstacle in evaluating river resources and or receiving reservoirs, dams, estuaries, and lakes.

In the case of limited gauges within a watershed, e.g., a single gauge in the Isahaya Reservoir watershed without available hydrologic information, direct regionalization of such discharge information to the ungauged site could be erratic and unreliable. This is due to differences in gradient, land use, soils, weather conditions, catchment area, and river basin shape. Therefore, the new framework presented in this study contributes to the hydrologic characterization of watersheds that have a limited number of gauges. Based on the differences in land use, slope, and size of the Isahaya Reservoir catchment, the new framework showed consistency and reliability in transplanting flow dynamics to the ungauged site.

In the Isahaya Reservoir watershed, differences in the river basins are not considered extreme. Therefore, further studies need to be conducted to determine the applicability of the new framework in cases where the donor and recipient river basins are vastly different. In addition, the framework should be further developed for watersheds with different weather conditions and subsurface hydrologic conditions. Depending on the assumptions made for this study, the applicability of the new framework was successful in the Isahaya catchment. This provides a flow regime for 10 river basins that would form the basis for further basin and/or water quality analyses. While this study does not provide an exclusive method for transplanting flow signatures from gauged river basin to ungauged river basin, it does provide a reliable method for estimating and characterizing continuous flow rate in a watershed with limited gauging stations and relatively similar weather conditions.

Acknowledgements

Support for this work was provided by the Nagasaki University, Engineering department. Authors are thankful to Riverine laboratory members; Mr. Nakamura, Mr. Mukai, and others for helping with field observations and emotional support. Authors also appreciate Dr. Kilonzi for proofreading our work.

Conflicts of Interest

The authors declare no conflicts of interest regarding the publication of this paper.

References

[1] Marahatta, S., Devkota, L.P. and Aryal, D. (2021) Application of Swat in Hydrological Simulation of Complex Mountainous River Basin (Part I: Model Development), *Water* (*Switzerland*), **13**, Article 1546. https://doi.org/10.3390/w13111546

[2] Nkwasa, A., Chawanda, C.J., Msigwa, A., Komakech, H.C., Verbeiren, B. and van Griensven, A. (2020) How Can We Represent Seasonal Land Use Dynamics in SWAT and SWAT + Models for African Cultivated Catchments. *Water* (*Switzerland*), **12**, Article 1541. https://doi.org/10.3390/w12061541

[3] Misigo, A.W.S. and Suzuki, S. (2018) Spatial-Temporal Sediment Hydrodynamics and Nutrient Loads in Nyanza Gulf, Characterizing Variation in Water Quality. *World Journal of Engineering and Technology*, **6**, 98-115. https://doi.org/10.4236/wjet.2018.62B009

[4] Gatwaza, O.C., Cao, X. and Beckline, M. (2016) Impact of Urbanization on the Hydrological Cycle of Migina Catchment, Rwanda. *Open Access Library Journal*, **3**, e2830. https://doi.org/10.4236/oalib.1102830

[5] Nruthya, K. and Srinivas, V.V. (2015) Evaluating Methods to Predict Streamflow at Ungauged Sites Using Regional Flow Duration Curves: A Case Study. *Aquatic Procedia*, **4**, 641-648. https://doi.org/10.1016/j.aqpro.2015.02.083

[6] Asurza-Véliz, F.A. and Lavado-Casimiro, W.S. (2020) Regional Parameter Estimation of the SWAT Model: Methodology and Application to River Basins in the Peruvian Pacific Drainage. *Water*, **12**, Article 3198. https://doi.org/10.3390/w12113198

[7] Ezemonye, M.N., Emeribe, C.N. and Anyadike, N.C.R. (2016) Estimating Stream Discharge of Aboine River Basin of Southeast Nigeria Using Modified Thornthwaite Climatic Water Balance Model. *Journal of Applied Sciences and Environmental Management*, **20**, 760-768. https://doi.org/10.4314/jasem.v20i3.30

[8] Swain, J.B. and Patra, K.C. (2017) Streamflow Estimation in Ungauged Catchments Using Regionalization Techniques. *Journal of Hydrology*, **554**, 420-433. https://doi.org/10.1016/j.jhydrol.2017.08.054

[9] Choubin, B., Solaimani, K., Rezanezhad, F., Roshan, M.H., Malekian, A. and Shamshirband, S. (2019) Streamflow Regionalization Using a Similarity Approach in Ungauged Basins: Application of the Geo-Environmental Signatures in the Karkheh River Basin, Iran. *Catena*, **182**, Article ID: 104128. https://doi.org/10.1016/j.catena.2019.104128

[10] Oudin, L., Andréassian, V., Perrin, C., Michel, C. and Le Moine, N. (2008) Spatial Proximity, Physical Similarity, Regression and Ungaged Catchments: A Comparison of Regionalization Approaches Based on 913 French Catchments. *Water Resources Research*, **44**, 1-15. https://doi.org/10.1029/2007WR006240

[11] Wagener, C.T., Blöschl, G., Goodrich, D.C., Gupta, H.V. and Sivapalan, M. (2012) A Synthesis Framework for Runoff Predictions in Ungauged Basins. In: Blöschl, G., Sivapalan, M., Wagener, T., Viglione, A. and Savenije, H., Eds., *Runoff Prediction in Ungauged Basins*: *Synthesis across Processes*, *Places and Scales*, Cambridge University Press, Cambridge, MA, 11-28. https://doi.org/10.1017/CBO9781139235761.005

[12] Sumioka, B.S., Kresch, D.L. and Kasnick, K.D. (2000) Magnitude and Frequency of

Floods in Washington. U.S. Geological Survey Water-Resources Investigation.

[13] Bisese, J. (1995) Methods for Estimating the Magnitude and Frequency of Peak Discharges of Rural, Unregulated Streams in Virginia. U.S. Geological Survey, Virginia. https://pubs.usgs.gov/wri/wri944148/pdf/wrir_94-4148.pdf

[14] Yu, P.-S. and Yang, T.-C. (2000) Using Synthetic Flow Duration Curves for Rainfall-Runoff Model Calibration at Ungauged Sites. *Hydrological Processes*, **14**, 117-133. https://doi.org/10.1002/(SICI)1099-1085(200001)14:1<117::AID-HYP914>3.0.CO;2-Q

[15] Kim, D., Jung, I.W. and Chun, J.A. (2017) A Comparative Assessment of Rainfall-Runoff Modelling against Regional Flow Duration Curves for Ungauged Catchments. *Hydrology and Earth System Sciences*, **21**, 5647-5661. https://doi.org/10.5194/hess-21-5647-2017

[16] Arsenault, R. and Brissette, F.P. (2014) Continuous Streamflow Prediction in Ungauged Basins: The Effects of Equifinality and Parameter Set Selection on Uncertainty in Regionalization Approaches. *Water Resources Research*, **50**, 6135-6153. https://doi.org/10.1002/2013WR014898

[17] Poissant, D., Arsenault, R. and Brissette, F. (2017) Impact of Parameter Set Dimensionality and Calibration Procedures on Streamflow Prediction at Ungauged Catchments. *Journal of Hydrology*: *Regional Studies*, **12**, 220-237. https://doi.org/10.1016/j.ejrh.2017.05.005

[18] Arsenault, R., Breton-Dufour, M., Poulin, A., Dallaire, G. and Romero-Lopez, R. (2019) Streamflow Prediction in Ungauged Basins: Analysis of Regionalization Methods in a Hydrologically Heterogeneous Region of Mexico. *Hydrological Sciences Journal*, **64**, 1297-1311. https://doi.org/10.1080/02626667.2019.1639716

[19] Gubernick, R., Cenderelli, D., Bates, K., Johanson, D. and Jackson, S. (2008) Stream Simulation: An Ecological Approach to Providing Passage for Aquatic Organisms at Road-Stream Crossings, 646.

[20] Yilmaz, M.U. and Onoz, B. (2017) A Blended Approach For Streamflow Estimation at Ungauged Sites in Turkey. 1*st International Conference on Engineering Technology and Applied Sciences*, Afyonkarahisar, 21-22 April 2016, Turkey.

[21] Levin, S.B. and Farmer, W.H. (2020) Evaluation of Uncertainty Intervals for Daily, Statistically Derived Streamflow Estimates at Ungaged Basins across the Continental U.S. *Water* (*Switzerland*), **12**, Article 1390. https://doi.org/10.3390/w12051390

[22] Samuel, J., Coulibaly, P. and Metcalfe, R.A. (2011) Estimation of Continuous Streamflow in Ontario Ungauged Basins: Comparison of Regionalization Methods. *Journal of Hydrology Engineering*, **16**, 447-459. https://doi.org/10.1061/(ASCE)HE.1943-5584.0000338

[23] Abimbola, O.P., Wenninger, J., Venneker, R. and Mittelstet, A.R. (2017) The Assessment of Water Resources in Ungauged Catchments in Rwanda. *Journal of Hydrology*: *Regional Studies*, **13**, 274-289. https://doi.org/10.1016/j.ejrh.2017.09.001

[24] Fan, F., Deng, Y., Hu, X. and Weng, Q. (2013) Estimating Composite Curve Number Using an Improved SCS-CN Method with Remotely Sensed Variables in Guangzhou, China. *Remote Sensing*, **5**, 1425-1438. https://doi.org/10.3390/rs5031425

[25] Abbaspour, K.C., Rouholahnejad, E., Vaghefi, S., Srinivasan, R., Yang, H. and Kløve, B. (2015) A Continental-Scale Hydrology and Water Quality Model for Europe: Calibration and Uncertainty of a High-Resolution Large-Scale SWAT Model. *Journal of Hydrology*, **524**, 733-752. https://doi.org/10.1016/j.jhydrol.2015.03.027

[26] Bai, P., Liu, X. and Liu, C. (2018) Improving Hydrological Simulations by Incorporating GRACE Data for Model Calibration. *Journal of Hydrology*, **557**, 291-304. https://doi.org/10.1016/j.jhydrol.2017.12.025

[27] Seiller, G., Anctil, F. and Perrin, C. (2012) Multimodel Evaluation of Twenty Lumped Hydrological Models under Contrasted Climate Conditions. *Hydrology and Earth System Sciences*, **16**, 1171-1189. https://doi.org/10.5194/hess-16-1171-2012

[28] Patil, S. (2011) Information Transfer for Hydrologic Prediction in Ungauged River Basins. Ph.D. Thesis, Georgia Institute of Technology, Atlanta.

[29] Razavi, T. and Coulibaly, P. (2013) Streamflow Prediction in Ungauged Basins: Review of Regionalization Methods. *Journal of Hydrologic Engineering*, **18**, 958-975. https://doi.org/10.1061/(ASCE)HE.1943-5584.0000690

[30] Strömqvist, J., Arheimer, B., Dahné, J., Donnelly, C. and Lindström, G. (2012) Prévisions des débits et des nutriments dans les bassins non jaugés: Mise en place et évaluation d'un modèle à l'échelle nationale. *Hydrological Sciences Journal*, **57**, 229-247. https://doi.org/10.1080/02626667.2011.637497

[31] Hrachowitz, M., Savenije, H.H.G., Blöschl, G., McDonnell, J.J., Sivapalan, M., Pomeroy, J.W., *et al.* (2013) A Decade of Predictions in Ungauged Basins (PUB)-A Review. *Hydrological Sciences Journal*, **58**, 1198-1255. https://doi.org/10.1080/02626667.2013.803183

[32] Parajka, J., Merz, R. and Blöschl, G. (2005) A Comparison of Regionalisation Methods for Catchment Model Parameters. *Hydrology and Earth System Sciences*, **9**, 157-171. https://doi.org/10.5194/hess-9-157-2005

[33] Arnold, J.G., Srinivasan, R., Muttiah, R.S. and Williams, J.R. (1998) Large Area Hydrologic Modeling and Assessment Part I: Model Development. *Journal of the American Water Resources Association*, **34**, 73-89. https://doi.org/10.1111/j.1752-1688.1998.tb05961.x

[34] Srinivasan, R., Ramanarayanan, T., Arnold, J.G. and Bednarz, S. (1998) Large Area Hydrologic Modeling And Assessment Part II: Model Application. *Journal of the American Water Resources Association*, **34**, 91-101. https://doi.org/10.1111/j.1752-1688.1998.tb05962.x

[35] Koycegiz, C. and Buyukyildiz, M. (2019) Calibration of SWAT and Two Data-Driven Models for a Data-Scarce Mountainous Headwater in Semi-Arid Konya Closed Basin. *Water*, **11**, Article 147. https://doi.org/10.3390/w11010147

[36] Van Liew, M.W. and Mittelstet, A.R. (2018) Comparison of Three Regionalization Techniques for Predicting Streamflow in Ungaged Watersheds in Nebraska, USA Using SWAT Model. *International Journal of Agricultural and Biological Engineering*, **11**, 110-119. https://doi.org/10.25165/j.ijabe.20181103.3528

[37] Pagliero, L., Bouraoui, F., Diels, J., Willems, P. and McIntyre, N. (2019) Investigating Regionalization Techniques for Large-Scale Hydrological Modeling. *Journal of Hydrology*, **570**, 220-235. https://doi.org/10.1016/j.jhydrol.2018.12.071

[38] Mitsugi, Y., Vongthanasunthorn, N., Mishima, Y., Koga, K., *et al.* (1967) Long-Term Change of Water Quality in the Reservoir of the Isahaya Bay Reclamation Project. *Lowland Technology International*, **15**, 21-28.

[39] Ittisukananth, P., Koga, K. and Vongthanasunthorn, N. (2008) Study on Algal Growth in Isahaya Reservoir. *Lowland Technology International*, **10**, 68-75.

[40] Central Environment Council (2015) Report on Assessment of Impacts of Climate Change in Japan and Future Challenges.

https://www.env.go.jp/en/focus/docs/files/20150300-100.pdf.

[41] Chaffe, P.L.B., Takara, K., Yamashiki, Y., Apip, Luo, P., Silva, R.V. and Nakakita, E. (2013) Cartographie des régions du Japon sensibles aux changements de la couverture nivale. *Hydrological Sciences Journal*, **58**, 1718-1728. https://doi.org/10.1080/02626667.2013.839874

[42] Mehan, S., Neupane, R.P. and Kumar, S. (2017) Coupling of SUFI 2 and SWAT for Improving the Simulation of Streamflow in an Agricultural Watershed of South Dakota. *Hydrology Current Research*, **8**, Article ID: 1000280. https://doi.org/10.4172/2157-7587.1000280

[43] Gitau, M.W. and Chaubey, I. (2010) Regionalization of SWAT Model Parameters for Use in Ungauged Watersheds. *Water* (*Switzerland*), **2**, 849-871. https://doi.org/10.3390/w2040849

[44] Fulford, J.M. and Sauer, V.B. (1986) Comparison of Velocity Interpolation Methods for Computing Open-Channel Discharge. Selected Papers in the Hydrologic Sciences. *Geological Survey Water-Supply Paper*, **2290**, 139-144.

[45] Krause, P., Boyle, D.P. and Bäse, F. (2005) Comparison of Different Efficiency Criteria for Hydrological Model Assessment. *Advances in Geosciences*, **5**, 89-97. https://doi.org/10.5194/adgeo-5-89-2005

[46] Muleta, M.K. (2012) Model Performance Sensitivity to Objective Function during Automated Calibrations. *Journal of Hydrologic Engineering*, **17**, 756-767. https://doi.org/10.1061/(ASCE)HE.1943-5584.0000497

[47] Faramarzi, M., Srinivasan, R., Iravani, M., Bladon, K.D., Abbaspour, K.C., Zehnder, A.J.B. and Goss, G.G. (2015) Setting up a Hydrological Model of Alberta: Data Discrimination Analyses Prior to Calibration. *Environmental Modelling & Software*, **74**, 48-65. https://doi.org/10.1016/j.envsoft.2015.09.006

[48] Sikorska, A.E., Del Giudice, D., Banasik, K. and Rieckermann, J. (2015) The Value of Streamflow Data in Improving TSS Predictions-Bayesian Multi-Objective Calibration. *Journal of Hydrology*, **530**, 241-254. https://doi.org/10.1016/j.jhydrol.2015.09.051

[49] Massmann, C. (2020) Identification of Factors Influencing Hydrologic Model performance Using a Top-Down Approach in a Large Number of U.S. Catchments. *Hydrological Processes*, **34**, 4-20. https://doi.org/10.1002/hyp.13566

[50] Bulygina, N., McIntyre, N. and Wheater, H. (2011) Bayesian Conditioning of a Rainfall-Runoff Model for Predicting Flows in Ungauged Catchments and under Land Use Changes. *Water Resources Research*, **47**, 1-13. https://doi.org/10.1029/2010WR009240

[51] Monjardin, C.E.F., Uy, F.A.A. and Tan, F.J. (2017) Estimation of River Discharge at Ungauged Catchment Using GIS Map Correlation Method as Applied in Sta. Lucia River in Mauban, Quezon, Philippines. *IOP Conference Series*: *Materials Science and Engineering*, **216**, Article ID: 012045. https://doi.org/10.1088/1757-899X/216/1/012045

[52] Parajka, J., Viglione, A., Rogger, M., Salinas, J.L., Sivapalan, M. and Blöschl, G. (2013) Comparative Assessment of Predictions in Ungauged Basins-Part 1: Runoff-Hydrograph Studies. *Hydrology and Earth System Sciences*, **17**, 1783-1795. https://doi.org/10.5194/hess-17-1783-2013

[53] Loukas, A. and Vasiliades, L. (2014) Streamflow Simulation Methods for Ungauged and Poorly Gauged Watersheds. *Natural Hazards and Earth System Sciences*, **14**, 1641-1661. https://doi.org/10.5194/nhess-14-1641-2014

[54] Rajib, M.A., Merwade, V. and Yu, Z. (2016) Multi-Objective Calibration of a Hydrologic Model Using Spatially Distributed Remotely Sensed/*in-Situ* Soil Moisture. *Journal of Hydrology*, **536**, 192-207. https://doi.org/10.1016/j.jhydrol.2016.02.037

[55] Siderius, C., Biemans, H., Kashaigili, J.J. and Conway, D. (2018) Going Local: Evaluating and Regionalizing a Global Hydrological Model'S Simulation of River Flows in a Medium-Sized East African Basin. *Journal of Hydrology*: *Regional Studies*, **19**, 349-364. https://doi.org/10.1016/j.ejrh.2018.10.007

[56] Kouchi, D.H., Esmaili, K., Faridhosseini, A., Sanaeinejad, S.H., Khalili, D. and Abbaspour, K.C. (2017) Sensitivity of Calibrated Parameters and Water Resource Estimates on Different Objective Functions and Optimization Algorithms. *Water* (*Switzerland*), **9**, Article 384. https://doi.org/10.3390/w9060384

[57] Bock, A.R., Farmer, W.H. and Hay, L.E. (2018) Quantifying Uncertainty in Simulated Streamflow and Runoff from a Continental-Scale Monthly Water Balance Model. *Advances in Water Resources*, **122**, 166-175. https://doi.org/10.1016/j.advwatres.2018.10.005

[58] Pokorny, S., Stadnyk, T.A., Ali, G., Lilhare, R., Déry S.J. and Koenig, K. (2021) Cumulative Effects of Uncertainty on Simulated Streamflow in a Hydrologic Modeling Environment. *Elementa*: *Science of the Anthropocene*, **9**, Article 431. https://doi.org/10.1525/elementa.431

[59] Hamilton, A.S. and Moore, R.D. (2012) Quantifying Uncertainty in Streamflow Records. *Canadian Water Resources Journal*, **37**, 3-21. https://doi.org/10.4296/cwrj3701865

[60] Lee, K., Ho, H.-C., Marian, M. and Wu, C.-H. (2014) Uncertainty in Open Channel Discharge Measurements Acquired with StreamPro ADCP. *Journal of Hydrology*, **509**, 101-114. https://doi.org/10.1016/j.jhydrol.2013.11.031

[61] Huang, H. (2012) Uncertainty Model for In Situ Quality Control of Stationary ADCP Open-Channel Discharge Measurement. *Journal of Hydraulic Engineering*, **138**, 4-12. https://doi.org/10.1061/(ASCE)HY.1943-7900.0000492

[62] WMO (2017) Guidelines for the Assessment of Uncertainty for Hydrometric Measurement.

Appendix

Appendix 1. Derivation of Equation (2)

Different land use influence characteristics of the daily flow rate at discharge point differently. The Characteristic of the hydrograph is the summation of partitioned individual land uses within the watershed. Within river basins in Isahaya catchment, Urban High-Density Land Use had no substantive influence on the characteristics of the mean daily flow rate. Agricultural lands (rice fields, and range bush (citrus fruits bush,)) which are major human activities in the catchment, and the forests (deciduous, Evergreen, and mixed) had a significant influence on the daily mean discharge for all the river basins. Arbitrary letting,

1) Q_F—Portion of discharge influenced by/from forest cover;

2) Q_H—Portion of discharge influenced by/from human activities related to the land use;

3) Q_U—Portion of discharge influenced by/from a fraction of watershed that is under Urban High Density;

4) Q_B—Portion of discharge influenced by/from a fraction of watershed that is **set** to barren during scenario simulations;

5) k—A fraction of watershed under Urban High Density/barren land use (only defined in scenario contest; was not among land use in the catchment).

Let the total discharge Q at the exit of the river be influenced by three land-uses as

$$Q = Q_F + Q_H + Q_U \tag{a}$$

In a scenario where a section of Forest or Human activities land use is changed to barren, then change in the total discharge was arbitrarily defined as

$$\Delta Q = Q_H + Q_F + Q_U - Q_{B^*} \tag{b}$$

Given that the influence of Q_U is negligible within the study catchment, the urban area was assumed to have a similar influence on the hydrographs as barren land cover with respect to the definition and use of the formula. The Equation (b) was then rewritten as

$$\Delta Q = Q_H + Q_F + kQ_{B^*} - Q_{B^*} \tag{c}$$

where, k is a fraction of the watershed under urban high density and/or barren if so defined. The difference in discharge at time T (days) was defined by Equation (c) that could be re-written as

$$Q_T = Q_F + Q_H - (1-k)Q_B \tag{d}$$

where $Q_B \neq 0$. At minimum before cosidering any of the three scernarios $Q_{B^*} = Q_U$

Based on the scenarios in this study, the daily mean discharge is approximately equal to the Q_T as defined in Equation (d). The above equation Eqn.d. formed an integral part of the correction factor ratio C_f.

Appendix 2. Calculation of the Uncertainty in Flow Measurement

The following are some of the sources of the uncertainties involved in the estimation of the final discharge estimate.

1) Instrumental resolution

This entails a value corresponding to half of the last significant digit of the software output for velocity (0.001 m/s). The user has no capability to making any record beyond the last significant digit and primarily depends on digits outputted from the software. The same applies to the measuring tape and wading road; the last significant digit that can be read by the user.

2) Instrument accuracy

This was based on the manufacturers' specifications for the instrument accuracy of ±2%/FS (±0.01 m/s). The accuracy is specified as % FS hence the error is applied as a fixed value no matter the output. During calibration of the machine and test in the laboratory, the precision was determined as ±1 cm/s. Using fine laboratory measurement and the use of the wading rod in the determination of depth, a discrepancy of ±0.001 and ±0.015 was noticed respectively.

3) Exposure/averaging time

These are fluctuations that appear as random noise in measurements taken by an instrument with high-frequency sampling capabilities such as the Kenek VPT-200-24. The "noise" is majorly due to flow turbulence. Other sources of such noise that could accumulate in the output signal due to instrument noise (electronic noise, Doppler noise), and environmental noise (wave effects, erratic operations by person). To make one observation at a given locale, the machine was set to 40 seconds for numerous samplings and then recorded output as averages. Records taken at a single point (continuous records, 40 seconds and reset for new reading) indicated average differences of 0.25% **Table 6**. (in the main text) summarizes the uncertainty sources associated with the stream discharge measurement using Kenek VPT-200-24 [59] [60].

4) Flow angle induced error

This is a flow-angle error due to incorrect inclination to flow and during calibration of the compass being used. The error was estimated as the manufacturer's specification of ±3˚/360˚ for the calibrated flow meter. This is an important error to be considered since it causes overestimation in sub-section discharge, respectively as discussed by Huang, 2012 [61]. The inclination of the machine was adjusted in each point velocity before the determination of the discharge. However, the flow angle error arising from calibration was not considered as the instrument was well calibrated before use. It was assumed that the error was less than 1% thus negligible.

5) Operational conditions

This error is because of the non-uniformity of suspended scatters in the electromagnet beams, change in flow direction during measurement, machine deflections, disturbance of the water surface by waves, and operator-induced effects. This is influenced by procedures used in field measurements and/or natural

conditions during measurement [62]. Ten repeated measurements at the same vertical were made in the field experiment to try and quantify this type A error for the flow meter. Using a wadding rod for measuring the depth, angle inclination, positioning of riverbed and miss-readings are some of the errors that could be incurred in field observation. Considering measurement at the same location by several users, the error was defined. The standard uncertainty associated with the main measured variables (mean velocity in the vertical, depth, and width) were then aggregated through the following relationships (scripts defined in **Table 5**):

$$u\left(\bar{v}_n\right)=\sqrt{u\left(\bar{v}_{re}\right)^2+u\left(\bar{v}_{ac}\right)^2+u\left(\bar{v}_{et}\right)^2+u\left(\bar{v}_{op}\right)^2} \tag{e}$$

$$u\left(d_n\right)=\sqrt{u\left(d_{re}\right)^2+u\left(d_{ac}\right)^2+u\left(d_{op}\right)^2} \tag{f}$$

$$u\left(b_n\right)=\sqrt{u\left(b_{re}\right)^2+u\left(b_{op}\right)^2} \tag{g}$$

The standard uncertainty for the measured discharges of R-8 (example) obtained with Equation (e) was expressed as combined standard uncertainty as:

$$u_c\left(Q_t\right)=\sqrt{\sum_{n-1}^{10}u\left(\bar{v}_n\right)^2\left(\frac{\partial Q_t}{\partial \bar{v}_n}\right)^2+\sum_{n-1}^{10}u\left(d_n\right)^2\left(\frac{\partial Q_t}{\partial d_n}\right)^2+\sum_{n-1}^{10}u\left(b_n\right)^2\left(\frac{\partial Q_t}{\partial b_n}\right)^2} \tag{h}$$

The contribution of the correlated uncertainties in two width measurements in the sub-area was assumed to be zero for this research.

For a sub area discharge at the n^{th} measurement, the functional relationship was defined as [62]:

$$q_i=\frac{1}{2}\left(b_{n+1}-b_{n-1}\right)d_n\bar{v}_i \tag{i}$$

Sensitivity coefficients, c, for each input were found by taking the partial derivatives for each independent variable in the above equation:

$$\frac{\partial Q_t}{\partial \bar{v}_n}=c_{vn}=\frac{1}{2}\left(b_{n+1}-b_{n-1}\right)d_n \tag{j}$$

$$\frac{\partial Q_t}{\partial d_n}=c_{dn}=\frac{1}{2}\left(b_{n+1}-b_{n-1}\right)\bar{v}_n \tag{k}$$

$$\frac{\partial Q_t}{\partial b_n}=c_{bn}=\frac{1}{2}\bar{v}_n d_n \tag{l}$$

Combined standard uncertainty was then defined as

$$u_c\left(Q_t\right)=\sqrt{\sum_{n-1}^{10}c_{vn}^2u\left(\bar{v}_n\right)^2+\sum_{n-1}^{10}c_{dn}^2u\left(d_n\right)^2+\sum_{n-1}^{10}c_{bn}^2u\left(b_n\right)^2} \tag{m}$$

The expanded uncertainty was determined as follows.

$$U\left(Q_t\right)=ku_c\left(Q_t\right) \tag{n}$$

The coverage factor of $k=2$ was adopted corresponding to normal distribution giving the estimate a 95% confidence interval. **Table 7** shows the uncer-

tainty that was possibly propagated during flow measurement within the study period. The seasons determined how many sub-sections could be undertaken throughout the research time.